Journal of Intelligent & Robotic Systems (2024) 110:70
https://doi.org/10.1007/s10846-024-02098-z

SHORT PAPER

Simultaneous and Independent Control of Multiple Swimming Magnetic Microrobots by Stabilizer Microrobot

Ruhollah Khalesi[1] · **Hossein Nejat Pishkenari**[1] · **Gholamreza Vossoughi**[2]

Received: 2 February 2023 / Accepted: 9 April 2024 / Published online: 8 May 2024

Abstract
This paper presents a new strategy for simultaneous control of multiple magnetic Micro Robots (MRs) improving stability and robustness with respect to external disturbances. Independent control of multiple MRs, can enhance efficiency and allows for performing more challenging applications. In this study, we present a system consisting of a Helmholtz coil and 2N Permanent Magnets (PMs), rotated by servomotors, to control several MRs. We have also improved the system's stability by adding a larger MR (stabilizer MR). This MR can be moved all around the workspace and works as a moving internal magnetic field source. Thanks to this moveable magnetic field, other MRs are more stable against environmental disturbances. By simulating simultaneous and independent control of multiple MRs, we demonstrate the advantages of using the stabilizer MR (more than 20 percent reduction in tracking error and control effort). In addition, we evaluate experimentally our proposed method to independently control the position of three MRs using a stabilizer MR demonstrating the efficacy of the strategy.

Keywords Magnetic microrobots · Permanent magnet · Stabilizer microrobot · Simultaneous and independent control

1 Introduction

Small-scale robots, with dimension less than 1-mm, have been widely studied because of their amazing potential applications in different fields including medicine [1, 2], small-scale fabrication [3–5], sensors and wireless data transmission [6, 7]. By recent technological advancement, MRs will be manufactured in different dimensions and shapes [8–10]. For controlling MRs, various external energy sources have been used such as light [11, 12], acoustics [13–15], electric field [16] and charge [17], magnetic field [18–20], and their combination [21]. The magnetic field is the most commonly used actuation system, because it can penetrate body tissue without causing any side effects, and can be produced by different equipment such as permanent magnets and electromagnetic systems in a variety of ways such as rotating or oscillating fields [22, 23]. By controlling multiple MRs simultaneously, more complicated tasks with higher accuracy and speed can be done. However due to the small size of the workspace and the proximity of the MRs, control of multiple MRs is challenging. Furthermore, accurate control is difficult due to uncertainties in the system model and disturbances in the workspace.

Previously reported researches in the field of simultaneous control of MRs using magnetic fields can be divided into three categories. In the first group, the same control input applied to all MRs, but due to their different physical properties, their motion will be distinct. As these MRs responds differently to the applied magnetics field, simultaneous control is achievable with suitable design. In most papers, the movement of these MRs is not entirely independent and is influenced by the ratio of their physical characteristic [24, 25]. However, certain studies introduce techniques for achieving fully decoupled independent motion. These methods involve immobilizing all microrobots except the intended one, allowing for the exclusive movement of a single MR while the others remain fixed [26, 27]. The second category belongs to the MR control with customized surfaces which can create local fields and gradients. As an example, by employing an array of planar coils, one can move a specific MR while the other MRs remain stationary. This strategy is only suitable for two-dimensional movements [28–30].

✉ Hossein Nejat Pishkenari
nejat@sharif.edu

[1] Nanorobotics Laboratory, Department of Mechanical Engineering, Sharif University of Technology, Tehran, Iran

[2] Department of Mechanical Engineering, Sharif University of Technology, Tehran, Iran

In the third category, control inputs should be different at the position of each MR which is a challenging problem due to the proximity of the MRs. Despite the difficulties of this method, it does not have the drawbacks of earlier methods and can lead to a more accurate independent three-dimensional control of MRs. In the previous works in this category, usually two MRs are controlled in-plane [31, 32], and in cases where the movement is three-dimensional, the system is over-actuated, and the number of control inputs exceeds the system states. For example, Ungaro et al. [33] developed a system that uses nine electromagnetic coils to control two MRs in three dimensions. Another challenge in simultaneous control is inter-agent forces which is ignored in most cases. In [18], Yousefi et al. proposed a fully actuated setup to control two MRs independently and simultaneously using four rotating PMs in two dimensions. But the MRs were considered widely apart in this study, and the forces between them are ignored. In [34], to account for disturbances and the model's uncertainties, a sliding mode controller was introduced. In [35], Salehizadeh et al. controlled two MRs in three dimensions using the force between them. However, increasing the number of MRs in this method increases the inter-agent forces computations, and makes the simultaneous control very complicated.

Despite significant progress and efforts in the field of simultaneous control of MRs, this topic requires additional research due to its importance and numerous applications. Due to existence of external disturbances on the micro robots, despite controller performance, they easily exit from their desired positions. Furthermore, the field created by the PMs and electromagnetic coils is highly influenced by their distance from the workspace, and precise motions will be more difficult by increasing the distance. The main contribution of the present work is proposing a novel idea in the control of multiple MRs by adding a dummy microrobot which increases the stability of the MRs in keeping their positions. Moreover, by adding a larger MR with more magnetization relative to the main MRs, some advantages of using special surfaces such as having a controllable magnetic field source inside the workspace are achieved, which leads to an increase in the stability of the MRs and reduction in the control effort. Also, the number of control parameters is equal to the number of variables and the setup is fully actuated. Totally the proposed setup, improves the stability, reduces the control effort while decreasing the positioning error. The setup includes rotatable PMs that create the required magnetic field inside the workspace, and a Helmholtz coil that aligns MRs similarly. The PMs angles are determined based on some simple calculations, which speeds up the control loop. In summary, the main contribution of the present study is introducing and adding a stabilizer microrobot to the workspace to improve the control system performance. These improvements in the control system performance includes.

- Improvement of stability: the microrobots can remain in their desired position with higher stability and lower sensitivity to external disturbances. This also leads to lower positioning error where the simple microrobots can better follow their desired positions.
- Reduction of the control effort: the actuation system needs a lower energy consumption to perform a control scenario for positioning of the microrobots with respect to the case where the stabilizer microrobot is not present.

The paper is structed as follows. Section 2, introduces the setup, and describes the relations in general form. Also, the advantages of using stabilizer microrobot is described in this section. Section 3 presents the simultaneous and independent control of 4 MRs theoretically. In Section 4 experimental results of simultaneous control of three MRs are presented. This paper is concluded in last section.

2 System Description

Here, the design of the actuation system is explained, and the required relations and the control method are presented.

2.1 Setup Specification

A Helmholtz coil and rotating PMs are included in the suggested setup, and they are both symmetrically spaced out from the workspace's center, to ensure that all locations of the workspace have approximately the same condition for controllability to have uniform actuation of the microrobots throughout the workspace (Fig. 1). The advantage of using PMs to control MRs instead of electromagnetic coils is that the magnetic field and gradient can be increased regardless of temperature limitations [36]. In addition, a stabilizer MR is used to create a moving magnetic field source and provide a better control of local magnetic field. This stabilizer MR can create some additional stable equilibrium points inside the workspace. If all the MRs can be aligned in the same direction, it can be shown that the control of MRs will be much simpler. So, a Helmholtz coil is utilized to generate a magnetic field that is much higher than the ones generated by PMs, aligning MRs perpendicular to the plane.

The PMs' centers are on the horizontal two-dimensional workspace plane. They generate the desired magnetic field gradient to move MRs, while the Helmholtz coil fixes the MRs orientation.

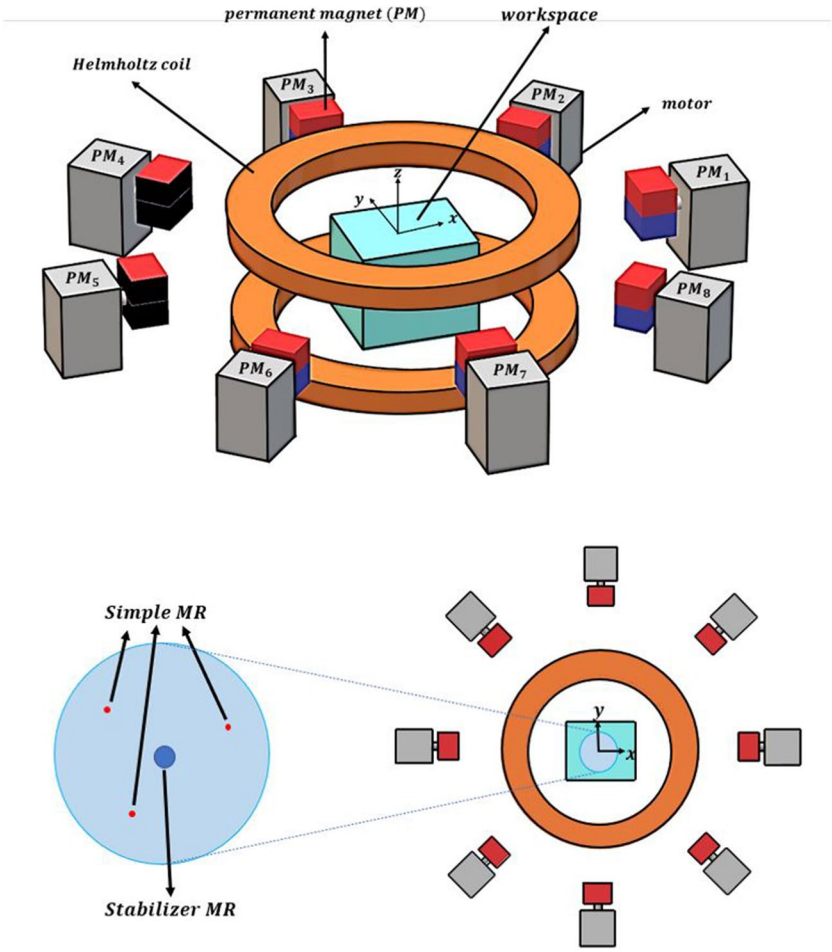

Fig. 1 The proposed setup for controlling multiple MRs consists of servomotors to rotate PMs and a pair of Helmholtz coils to align the MRs along the z-axis

2.2 Magnetic Field Relations

The magnet can be modeled as a simple dipole. For a cube-shaped PM at a distance twice its side length, the inaccuracy due to this approximation is less than 1% [37]. The following equations show the magnetic field vector ($\boldsymbol{B}$) and gradient matrix ($\boldsymbol{G}$) considering this simplification:

$$\boldsymbol{B} = \frac{\mu_0 \left|\boldsymbol{m}_{pm}\right|}{4\pi |\boldsymbol{r}|^3}(3\hat{\boldsymbol{r}}\hat{\boldsymbol{r}}^T - \boldsymbol{J})\hat{\boldsymbol{m}}_{pm} \tag{1}$$

$$\boldsymbol{G} = \frac{3\mu_0 \left|\boldsymbol{m}_{pm}\right|}{4\pi |\boldsymbol{r}|^4}(\hat{\boldsymbol{m}}_{pm}\hat{\boldsymbol{r}}^T + \hat{\boldsymbol{r}}\hat{\boldsymbol{m}}_{pm}^T - [5\hat{\boldsymbol{r}}\hat{\boldsymbol{r}}^T - \boldsymbol{J}](\hat{\boldsymbol{m}}_{pm}.\hat{\boldsymbol{r}})) \tag{2}$$

where μ_0 and $\boldsymbol{J}$ are the air permeability and the identity matrix respectively, $\boldsymbol{r}$ and $\hat{\boldsymbol{r}}$ are position vector, and its corresponding unit vector. $\boldsymbol{m}_{pm}$ and $\hat{\boldsymbol{m}}_{pm}$ are the PM magnetic moment, and its corresponding unit vectors. Magnetic force ($\boldsymbol{f}_m$) and torque ($\boldsymbol{\tau}_m$) can be calculated as follows:

$$\boldsymbol{f}_m = (\boldsymbol{m}_{mr}.\nabla)\boldsymbol{B} \tag{3}$$

$$\boldsymbol{\tau}_m = \boldsymbol{m}_{mr} \times \boldsymbol{B} \tag{4}$$

In these equations, $\boldsymbol{m}_{mr}$ is the MR magnetic moment. In the suggested setup, the Helmholtz coil aligns all the MRs by providing a large uniform field in comparison to the PMs magnet field. As a result, the force exerted on a particle with a magnetization of $\boldsymbol{m}_{mr}$ can be represented as:

$$\boldsymbol{f}_m = \left|\boldsymbol{m}_{mr}\right| \frac{[\boldsymbol{G}]\{\boldsymbol{B}\}}{|\boldsymbol{B}|} \tag{5}$$

2.3 Controller Design

Based on the presented equations, it can be deduced that if the PMs and the MRs are oriented in the same direction, each of the PMs repels the MR, resulting in a stable equilibrium point in the workspace. It is also possible to create the desired force at a specific point using the proposed setup. By increasing the number of the stable equilibrium points, controlling multiple MRs will be easier. This will be done by adding a small floating PM as a stabilizer

microrobot among the ordinary MRs. The position of the stabilizer MR is affected by the magnetic field, and this robot moves in the workspace due to the magnetic forces, but it should be noted that the stabilizer microrobot position is not directly controlled. In fact, its position remains uncontrolled, and it does not follow a predetermined trajectory. This MR has a higher magnetization than other MRs, and creates more stable equilibrium points in the workspace.

By defining l and $\varnothing_i$ as the PM distance from the workspace's center and its angle in respect to the x-axis, the position of each actuator in the cartesian coordinate can be represented by $[l.cos(\varnothing_i), l.sin(\varnothing_i), 0]$. Equation (5) can be employed to calculate exerted force by the first PM (with the orientation $[0, sin(\theta_1), cos(\theta_1)]$) on a MR located at $[x, y, 0]$ and oriented toward the z-axis as follows:

$$\boldsymbol{f}_{m,11} = |\boldsymbol{m}_{mr}|\boldsymbol{G}_{1,1}\begin{Bmatrix}0\\0\\1\end{Bmatrix} = \frac{3\mu_0|\boldsymbol{m}_{mr}|\left|\boldsymbol{m}_{pm}\right|}{4\pi}\frac{1}{|\boldsymbol{r}_{1,1}|^5}\begin{Bmatrix}(x-l).cos(\theta_1)\\ y.cos(\theta_1)\\ y.sin(\theta_1)\end{Bmatrix} \tag{6}$$

where θ_i and $\boldsymbol{r}_{i,j}$ are the rotation angle of the PM_i and the distance between PM_i and MR_j, and $\boldsymbol{G}_{i,j}$ and $\boldsymbol{f}_{m,ij}$ are the magnetic gradient and force on the MR_j by PM_i. By ignoring the z-axis forces due to the 2D motion constraint, the equation is rewritten as follows:

$$\boldsymbol{f}^{(xy)}_{m,11} = C_F\frac{1}{\left|\boldsymbol{r}^{(xy)}_{1,1}\right|^5}(\boldsymbol{r}^{(xy)}_{1,1})cos(\theta_1) \tag{7}$$

$$C_F = |\boldsymbol{m}_{mr}|\frac{3\mu_0\left|\boldsymbol{m}_{pm}\right|}{4\pi} \tag{8}$$

Superscripts *xy,* stands for the planar terms, and the C_F is the force coefficient. Rewriting this equation for all PMs results in the following formula, which can be used to calculate the magnetic force acting on the first MR:

$$\widetilde{\boldsymbol{f}}_m(\boldsymbol{p}_1) = \sum_{i=1}^{2\times N}\boldsymbol{f}^{(xy)}_{m,i1}(\boldsymbol{p}_1) = C_F\sum_{i=1}^{2\times N}\frac{u_i}{\left|\boldsymbol{r}^{(xy)}_{i,1}\right|^5}(\boldsymbol{r}^{(xy)}_{i,1}) \tag{9}$$

Here, N is the total number of simple MRs, and $2N$ is the total number of PMs based on the assumption that the system is fully actuated. u_i is the control parameter, and $\widetilde{\boldsymbol{f}}_m(\boldsymbol{p}_j)$ is the sum of the PM forces on the MR_j, which located at point $\boldsymbol{p}_j$ and oriented toward the z-axis. Each PMs rotation angle is converted to the control parameter as follows:

$$u_i = cos(\theta_i) \tag{10}$$

The magnetic force exerted by the PMs on the MRs can be expressed as follows by rewriting above relations for all the MRs:

$$\boldsymbol{F}_{PM}(\boldsymbol{p}_1,\boldsymbol{p}_2,\ldots,\boldsymbol{p}_N) = \boldsymbol{A}(\boldsymbol{p}_1,\boldsymbol{p}_2,\ldots,\boldsymbol{p}_N)\boldsymbol{u} \tag{11}$$

$$\boldsymbol{F}_{PM}(\boldsymbol{p}_1,\boldsymbol{p}_2,\ldots,\boldsymbol{p}_N) = \left[\widetilde{f}^{(x)}_m(\boldsymbol{p}_1)\ \widetilde{f}^{(y)}_m(\boldsymbol{p}_1)\ \ldots\ \widetilde{f}^{(x)}_m(\boldsymbol{p}_N)\ \widetilde{f}^{(y)}_m(\boldsymbol{p}_N)\ \right]^T \tag{12}$$

$$\boldsymbol{A} = C_F\begin{bmatrix}\frac{r^x_{1,1}}{|\boldsymbol{r}_{1,1}|^5} & \ldots & \frac{r^x_{1,2N}}{|\boldsymbol{r}_{2N,1}|^5}\\ \frac{r^y_{1,1}}{|\boldsymbol{r}_{1,1}|^5} & & \frac{r^y_{2N,1}}{|\boldsymbol{r}_{2N,1}|^5}\\ \vdots & \ddots & \vdots\\ \frac{r^x_{1,N}}{|\boldsymbol{r}_{1,N}|^5} & \ldots & \frac{r^x_{2N,N}}{|\boldsymbol{r}_{2N,N}|^5}\\ \frac{r^y_{1,N}}{|\boldsymbol{r}_{1,N}|^5} & & \frac{r^y_{2N,N}}{|\boldsymbol{r}_{2N,N}|^5}\end{bmatrix} \tag{13}$$

$$\boldsymbol{u} = \left[\ u_1\ \ldots\ u_{2N}\ \right] \tag{14}$$

where, $\boldsymbol{u}_{2N\times1}$ and $\boldsymbol{A}_{2N\times2N}$ are the control vector, and the actuation matrix. $(\boldsymbol{F}_{PM})_{2N\times1}$ represents the total magnetic forces exerted on MRs in each direction, which represented by the x and y superscripts. The stabilizer MR also exerts a force ($\boldsymbol{F}_s$), which may be measured similarly to the force exerted by the PMs. Along with these forces, the MR also experiences drag force, which is a function of the fluid's viscosity and drag coefficient. This drag force ($\boldsymbol{f}_d$) in the low Reynolds condition is obtained as follows:

$$\boldsymbol{f}_d = -\mu\boldsymbol{K}\boldsymbol{v} \tag{15}$$

where μ is the fluid viscosity, $\boldsymbol{K}$ is the drag coefficients matrix, and $\boldsymbol{v}$ is MRs velocity. This equation can be rewritten for all MRs and limited in 2D similarly to magnetic force as follows:

$$\boldsymbol{F}_d = -C\left[\ v^x_1\ v^y_1\ \ldots\ v^x_N\ v^y_N\ \right] = -C\dot{\boldsymbol{X}} \tag{16}$$

In the above relation, $\dot{\boldsymbol{X}}_{2N\times1}$ is the time derivative of the position of the MRs, and $\boldsymbol{F}_d$ is the drag forces vector. In the low Reynolds regime, drag forces are superior and inertial forces can be neglected. By ignoring the forces between the simple MRs, the force equations can be written as follows:

$$\boldsymbol{F}_{PM} + \boldsymbol{F}_s + \boldsymbol{F}_d = 0 \rightarrow \boldsymbol{F}_{PM} = C\dot{\boldsymbol{X}} - \boldsymbol{F}_s \tag{17}$$

Current ($\boldsymbol{r}_j$) and desired ($\boldsymbol{r}_{des,j}$) positions of MRs are used to estimate the required force to move this MR toward its desired position ($\boldsymbol{f}_{des,j}$) using a PI controller as follows:

$$\boldsymbol{f}_{des,j} = C\dot{\boldsymbol{r}}_{des,j} + k_p(\boldsymbol{r}_{des,j} - \boldsymbol{r}_j) + k_i\int(\boldsymbol{r}_{des,j} - \boldsymbol{r}_j)dt \tag{18}$$

In the above relation, k_p and k_i are the controller coefficients. By writing this equation for each MR ($\boldsymbol{F}_{des}$), PMs angles can be obtained using Eq. (11) as follow:

$$\boldsymbol{u}_N = \boldsymbol{A}^{-1}\boldsymbol{F}_{des} \tag{19}$$

$$\boldsymbol{u}_0 = \left(\frac{\boldsymbol{m}_s}{\boldsymbol{m}_{pm}}\boldsymbol{A}\right)^{-1}\boldsymbol{F}_s \tag{20}$$

$$\boldsymbol{u} = \boldsymbol{\alpha}\boldsymbol{u}_N - \boldsymbol{u}_0 \tag{21}$$

In the above equations, $\boldsymbol{u}_N$ is the input required to create the desired force to compensate error and $\boldsymbol{u}_0$ is the input required to overcome the force of the stabilizer MR. The coefficient $\boldsymbol{\alpha}$ has been added in Eq. (21) to ensure that the results are in the range between -1 and + 1. If the value of $\boldsymbol{u}_N - \boldsymbol{u}_0$ is outside the assumed range, after the correction using $\boldsymbol{\alpha}$, the direction of the desired force will remain unchanged but its magnitude will be smaller.

When constructing these equations, we presupposed that all the parameters are well-known and that there is no environmental uncertainty. Furthermore, the interaction between simple MRs and their deviation from the z-axis are neglected. Since external disturbances and model uncertainties are unavoidable under practical conditions, a basic PI controller may not be sufficient. We address this problem by adding a stabilizer MR to the system to improve its stability.

2.4 Advantage of Using a Stabilizer MR

Using the stabilizing MR in the workplace has two main advantages. The first one is improving the system's stability and the second one is reducing the control effort. If there is no stabilizer MR in the workspace, any force disturbance can exit the MRs from their desired position. Also, the PMs need to rotate continually to return the MRs to their final positions, which will increase the control effort. Also, if all the MRs have reached the target point, then the actuating magnets must be adjusted in angular positions which do not exert any forces on the MRs. As a result, the MRs may move away from their target point due PMs angles error or by any disturbance force in the workspace. A stabilizer MR will add some stable equilibrium points. When the MRs approach the stabilizer MR or PMs, the repulsive force exerted on MRs increases to return them to their equilibrium point.

To determine the system's equilibrium points, the first step involves finding the position of the stabilizer microrobot within the workspace using Eq. (9). Then, by considering $\boldsymbol{F}_d = 0$, we can identify the remaining equilibrium points using Eq. (17). These equations exhibit a highly nonlinear nature. For example, when we have four perfectly aligned PMs in the z-direction, the stabilizer microrobot will rest at the center due to symmetric forces. If we wish to find the equilibrium point's location in presence of stabilizer MR, Eq. (17) can be rewritten as follows:

$$\boldsymbol{F}_{PM} + \boldsymbol{F}_s = 0 \rightarrow \begin{cases} x: C_F\left(\frac{\cos(A_1)}{B_1^2} + \frac{\cos(A_2)}{B_2^2} + \frac{\cos(A_3)}{B_3^2} - \frac{\cos(A_4)}{B_4^2} + \frac{m_s/m_{PM}\cos(A_5)}{B_5^2}\right) = 0 \\ y: C_F\left(\frac{\sin(A_1)}{B_1^2} + \frac{\sin(A_2)}{B_2^2} + \frac{\sin(A_3)}{B_3^2} - \frac{\sin(A_4)}{B_4^2} + \frac{m_s/m_{PM}\sin(A_5)}{B_5^2}\right) = 0 \end{cases} \tag{22}$$

$$\begin{aligned} A_1 &= tan^{-1}\left(\tfrac{y}{x+l}\right), B_1 = (l+x)^2 + y^2 \\ A_2 &= tan^{-1}\left(\tfrac{y-l}{x}\right), B_2 = x^2 + (l-y)^2 \\ A_3 &= tan^{-1}\left(\tfrac{y}{x-l}\right), B_3 = (l-x)^2 + y^2 \\ A_4 &= tan^{-1}\left(\tfrac{y+l}{x}\right), B_4 = x^2 + (l+y)^2 \\ A_5 &= tan^{-1}\left(\tfrac{y}{x}\right), B_5 = x^2 + y^2 \end{aligned} \tag{23}$$

The left-hand side of the second Eq. (22) represents the magnetic force exerted in the x and y-direction by the PMs and the stabilizer microrobot respectively. Finding analytical solutions for the equation to determine the values of x and y is challenging due to the presence of nonlinearity. As a result, we employ a numerical approach to identify the equilibrium points and forces within the workspace.

For better understanding, some simulations were conducted in the presence of four PMs and a stabilizer MR in the workspace. In this case, the magnetization of the PMs is considered 100 times that of the stabilizer MR ($m_s/m_{PM} = 0.01$) and their distance from the workspace center is $l = 20cm$. All PMs are at zero-angle and are exerting maximum force to MRs based on Eq. (7). The center is the equilibrium point because the PMs angles are equal, and the stabilizer MR will move to this location. After that, 8 more equilibrium points will be formed in the workspace by stabilizer MR. The position of these equilibrium points is depicted in the Fig. 2a. In this figure, the blue dot indicates the stabilizer MR and the cross symbols indicate locations where there is no force in the radial direction. As indicated in Fig. 2a, locus of such points is a circle. If the MRs are positioned on this circle, they will not move away from the closed curve, but rather toward equilibrium positions (points where no force will be applied to the MRs—blue circles). The unit vector of magnetic force applied to the MRs is displayed in the workspace in the second figure. The four equilibrium points on the x and y axes are unstable, while the four

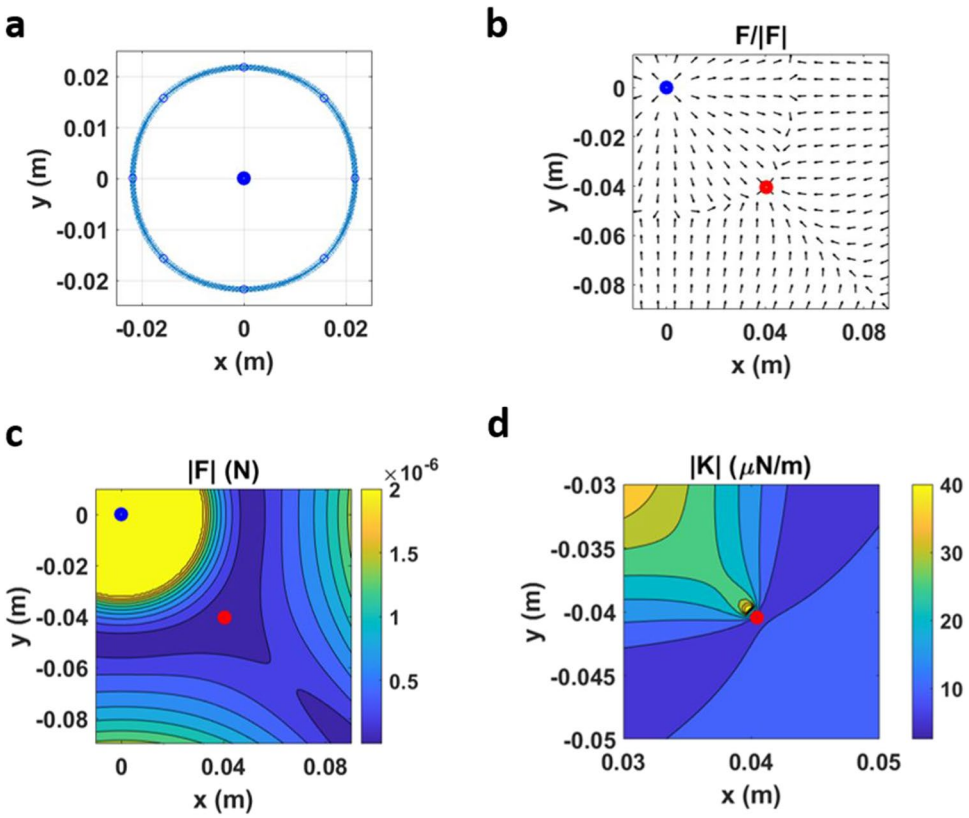

Fig. 2 The four PMs and a stabilizer MR simulation. (The Blue dot represents a stabilizer MR and the red one represents a simple MR) **a** equilibrium point **b** force field in the workspace. **c** force magnitude in the workspace. **d** equivalent spring coefficient of the system in the workspace

diagonal equilibrium points are stable. In general, it can be said that the equilibrium points on the stabilizer MR and the PMs cross line are unstable, because both the stabilizer MR and the PM forces are such that pushes the MRs away from these positions. The magnitude of the force in the workspace is also depicted in Fig. 2c. According to this figure, as one moves away from the equilibrium point, the magnitude of the forces increases. The corresponding spring coefficient is illustrated in Fig. 2d by dividing the force magnitude by the distance to the near equilibrium point. If the MRs move away from their equilibrium point, the existing force field returns them to the equilibrium position.

In the simulation section, it is shown that the presence of the stabilizer MR magnetic leads to the reduction of the control efforts. The equivalent spring coefficient for the equilibrium point in the workspace is obtained using force field and is as follows:

$$\boldsymbol{K}_{mat} = 10^{-3}\begin{bmatrix} 0.6226 & 0.5689 \\ 0.5689 & 0.6226 \end{bmatrix} N/m \tag{24}$$

This matrix is symmetric and positive definite and the eigenvalues of this matrix are 0.0001 and 0.0012, indicating the stability of the equilibrium point. The influence of the number of PMs and the stabilizer MR and PMs magnetization on the equilibrium point position is shown in the Fig. 3.

In this figure, β is the ratio of the stabilizer MR magnetization to the PMs magnetization, and γ is the distance between the stabilizer MR and the equilibrium point divided by the distance from the PM to the workspace center. According to the figure, by increasing the magnetization of the stabilizer MR, the distance between the equilibrium point and this MR will increase. Also, as the number of magnets increases, the force toward the center increases, and as a result, this distance decreases. Totally it can be deduced that the magnetization of the stabilizer MR is a design parameter to achieve the desired location of the equilibrium points.

Another benefit of utilizing a stabilizer MR is that it can improve the precision of adjusting the exerted force on the MRs. When a PM's angle is zero, the difference in force exerted by it when rotating a specific amount is at its highest. By adding a stabilizer MR, the PM should rotate to overcome this magnetic force. So, the force resolution applied to the MRs is reduced, and higher movement resolution can be achieved.

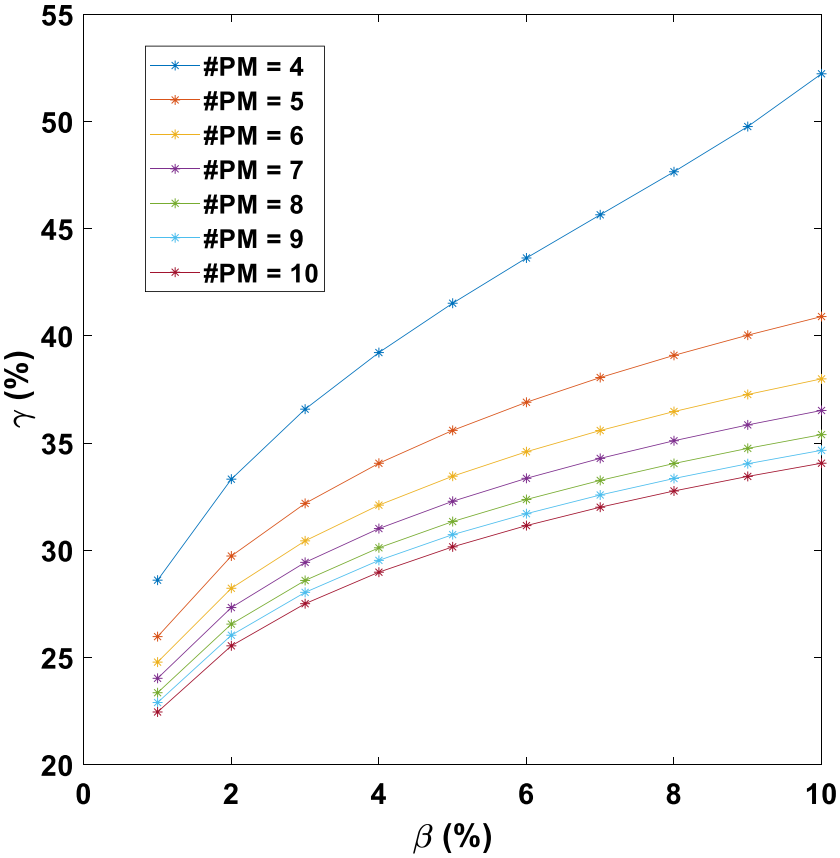

Fig. 3 The influence of the number of PMs and stabilizer MR and PM magnetization ratio (β) on distance between the stabilizer MR and the equilibrium point divided by the distance from the PM to the workspace center (γ)

3 Simulation

To evaluate the feasibility of the suggested concept, the simultaneous control of four MRs with eight PMs is simulated twice, with and without the stabilizer MR. If the stabilizer MR is not used, the relations are the same as in the previous section, with the exception that the influence of stabilizer MR is no longer considered. Table 1 shows the simulation parameters:

Table 1 Simulation parameters

Parameter	Value	Unit
Number of MRs	4 + 1	–
Number of PMs	8	–
PMs distance to workspace center	20	*cm*
MRs magnetization	1×10^{-4}	$A.m^2$
Stabilizer MR magnetization	8×10^{-2}	$A.m^2$
PMs magnetization	8	$A.m^2$
Winding magnetic field	10	*mT*
Radius of MRs	0.4	*mm*
Radius of stabilizer MR	1	*mm*
Fluid viscosity	0.01	*Pa.s*

Additionally, because of their disk form, the MRs' drag coefficient (C) is calculated as follows [38]:

$$C = \frac{16}{3}\mu d \tag{25}$$

d is the diameter of the disk. In the simulation, MRs move on the water surface. The rotation resolution is 0.01 degrees and the position determination precision is 0.1 mm. MRs track square shape trajectories, and all MRs have an initial error. The position of MRs along the path is shown in Fig. 4. As can be seen, using a stabilizer MR allows the other MRs correct their initial error faster. The stabilizer MR moves slightly with respect to the MRs, due to the higher drag coefficient.

Figure 5 indicates the PMs angles. As can be seen, the PMs were able to drive the MRs toward their target location by applying the magnetic field determined based on the analytical solution presented in the previous section. In

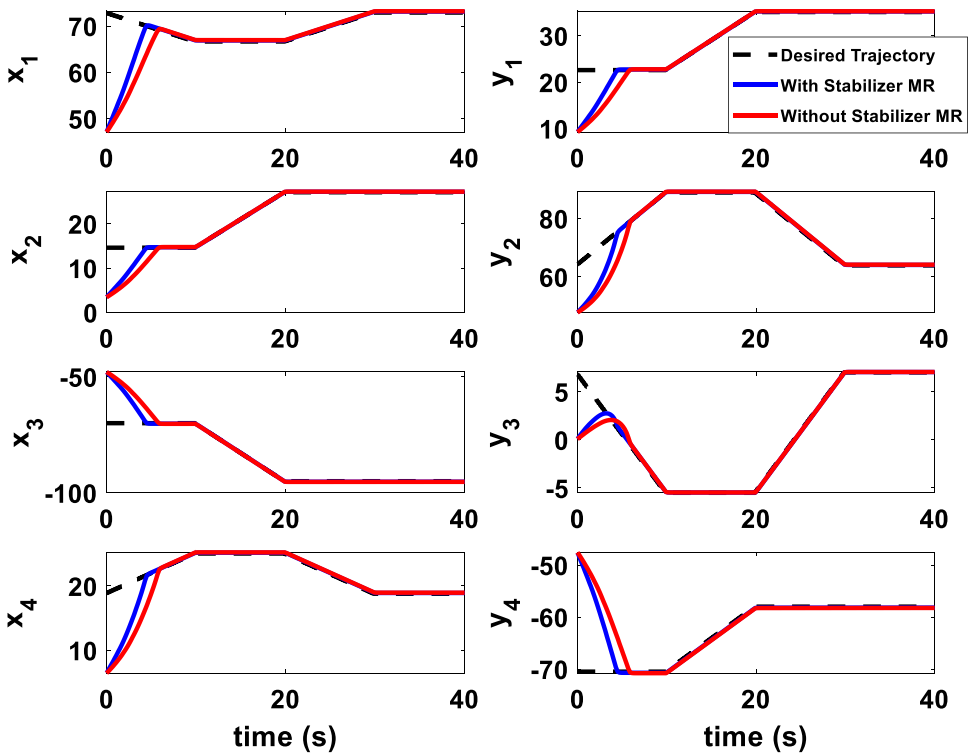

Fig. 4 Position of microrobots in simultaneous control of 4 microrobots with and without stabilizer microrobot

presence of the stabilizer MR, once the MRs reached their destinations, the PMs angles will be a value other than 90 degrees to compensate the force produced by the stabilizer MR. PM's angle oscillation is due to the resolution of the control of the servomotors angular position. In the presence of the stabilizer MR, the oscillation of PM angles reduces

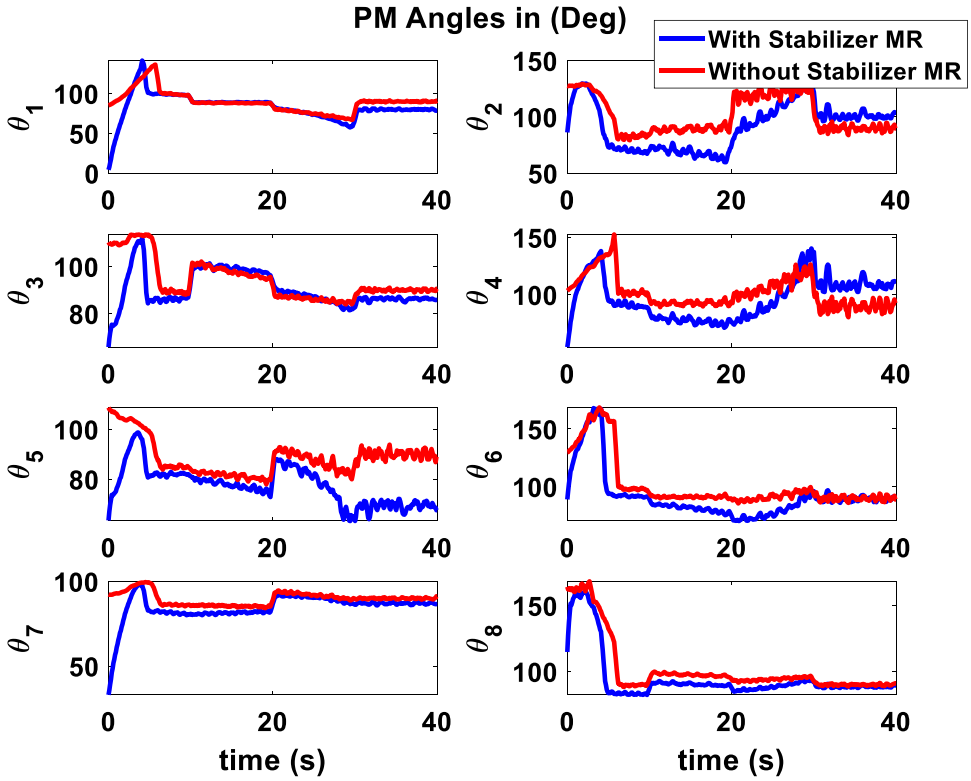

Fig. 5 Angles of permanent magnets in simultaneous control of 4 microrobots with and without stabilizer microrobot

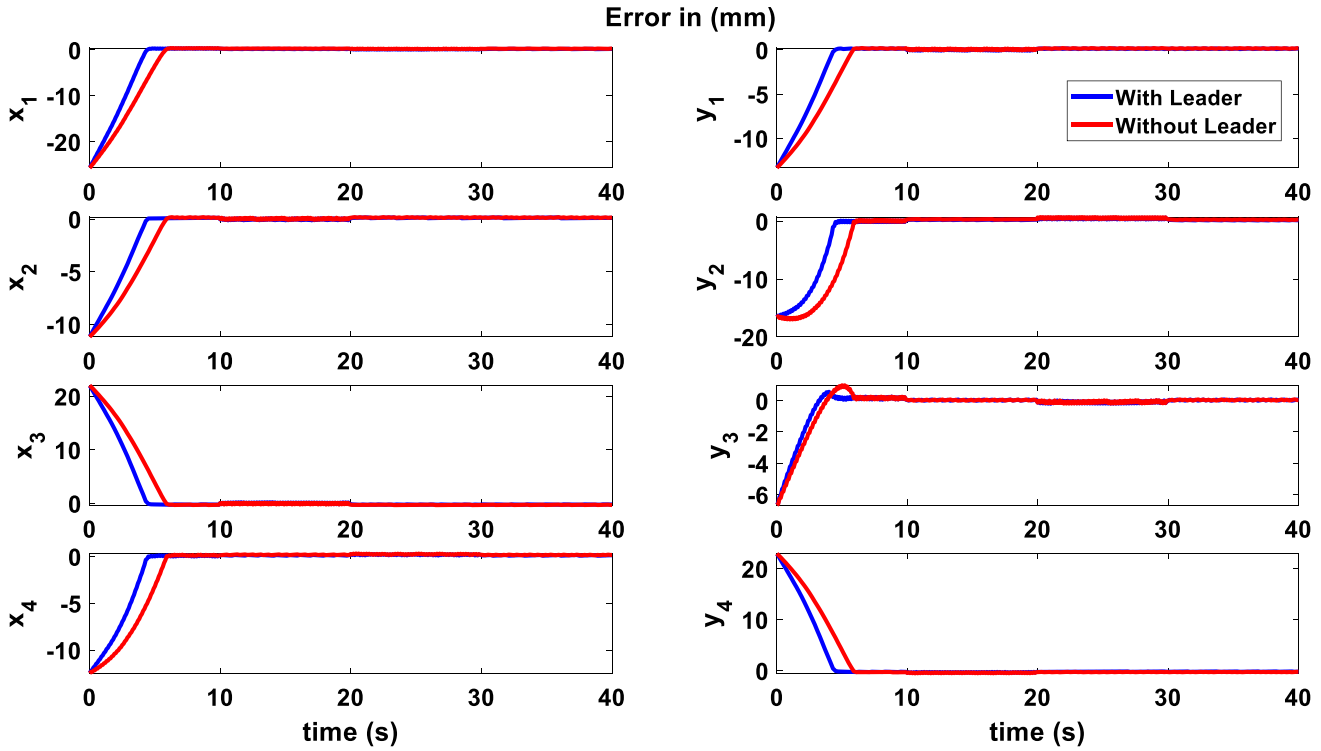

Fig. 6 Position error of microrobots in simultaneous control of 4 microrobots with and without stabilizer microrobot

since in this case an equilibrium zone around the MRs is formed. Figures 6 and 7 depict the error for each MR as well as the total tracking error. Despite the initial error, the MRs have successfully followed the desired trajectory. In addition, when a stabilizer MR is used, other MRs compensate their initial error more quickly.

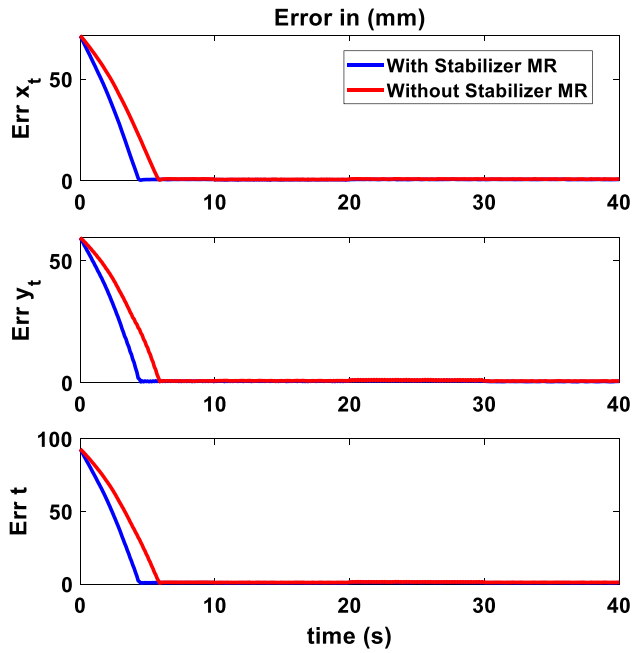

Fig. 7 Total positional error in simultaneous control of 4 microrobots with and without stabilizer microrobot

More details about the advantages of using a stabilizer MR are shown in Table 2. It can be seen that by using the stabilizer MR, the rise time and the control effort (integral of PMs angular velocity) will decrease about 25% and 22% respectively. Also, the stabilizer MR magnetic field increases the stability of the system and reduces the tracking and final error by 20% and 24% respectively.

It should be noted that these results are dependent on different parameters, such as MR and PM magnetization, MR drag coefficients, PM distance from workspace center, and travel path. If the path were set in such a way that

Table 2 Comparison of the effect of using stabilizer microrobot in simultaneous control simulation of 4 microrobots

Parameter	Unit	With stabilizer MR	Without stabilizer MR
Rise time	*s*	4.40	5.90
Control effort	–	6408.7	8162.7
Tracking error (after initial error compensation)	*mm*	0.98	1.23
Final position error	*mm*	0.85	1.12

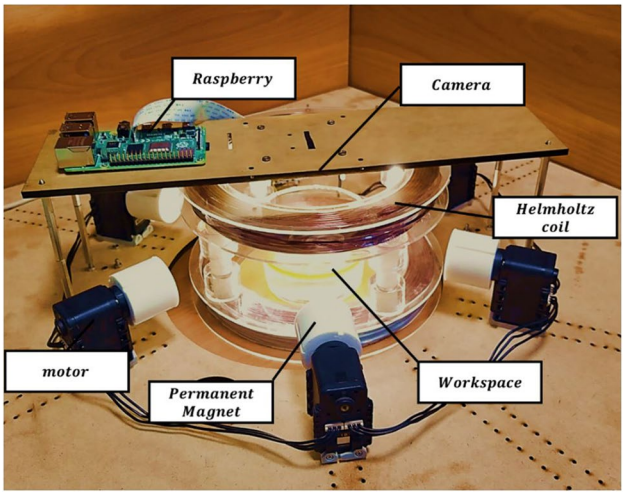

Fig. 8 Proposed setup for simultaneous control of three microrobots in a plane consists of six PMs and a Helmholtz coil

the MRs got closer to each other, more force would be required to overcome the stabilizer MR, and more control effort and time would be spent. For better illustration of the proposed method performance, a simulation for independent control of more MRs (12 MRs with 24 PMs) has been done, and the clip of these simulations is available in the supplementary material. Also, in the experiment section, three MRs have been controlled simultaneously to verify the idea with a different number of MRs.

4 Experiment

To assess the proposed method efficacy, we experimentally implemented the simultaneous control of three MRs ($N = 3$). The magnets are grade $N42$ and made of $NdFeB$ cubes with dimensions of $2Cm$ and are placed $12Cm$ away from the workplace center. The $DynamixelMX-12W$ servo motors are used to rotate the PMs. The position of the MRs is estimated from a camera mounted above the workspace, and a $RaspberryPi4$ board is used to calculate the required forces based on the PI controller. Then, PMs angles are obtained using the analytical solution, and by transmitting the necessary commands to servomotors, the closed-loop control system works. The control loop's frequency is $6Hz$, which is maximum achievable frequency in our setup to complete image processing. Due to MRs' slow motion, this frequency is adequate. The proposed setup and the structure of closed-loop motion control system are shown in Figs. 8 and 9 respectively. A Helmholtz coil with an average diameter of $30Cm$, 166 turns, and capability of creating a field of $10mT$, is used to align the MRs. Stabilizer MR is disk-shaped with a height and radius of $500\mu m$ and other MRs are cubes with a size of $250\mu m$ and both are made of neodymium.

In this experiment, water medium with a layer of oil on it was used. The stabilizer MR is put in the water–oil interface due to its higher density, and other MRs move on the oil surface. This difference increases the drag coefficient of the stabilizer MR and slows down its movement.

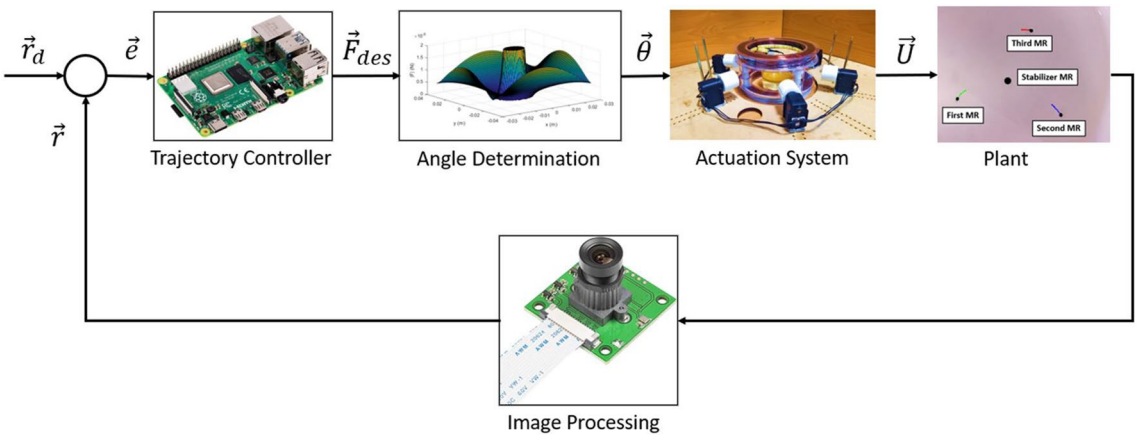

Fig. 9 Structure of closed-loop motion control system

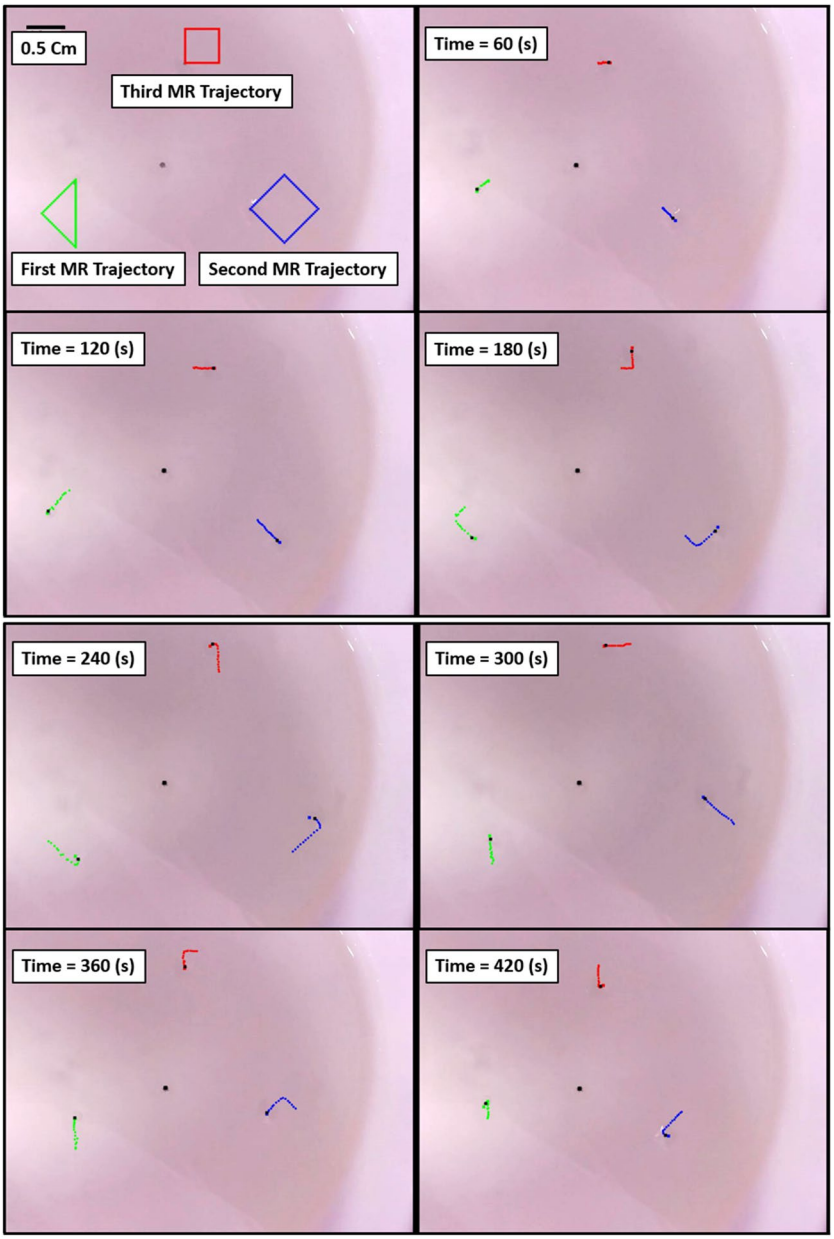

Fig. 10 Snapshot of the trajectories of microrobots in the test (desired trajectories are shown in the first image)

Figure 10 shows the path of the MRs. Two MRs travel clockwise on square and diamond paths, while the third travels counterclockwise on a triangle path. The MRs' initial position was selected randomly with different distances to the center of workspace, and the different desired trajectories were chosen to demonstrate the efficacy of the proposed method.

Figures 11 and 12 show the position and error of the path following. As can be seen, MRs follow their desired trajectories appropriately with mean square error 320 micron during test. Figure 13 shows the angles of the PMs. Based on this figure, PMs repel and attract MRs during the test.

The variety of paths and the low error in displacement indicate the efficacy of the proposed method. According to the results, simultaneous and independent control of MRs using a stabilizer MR in the workplace is conceivable, but the magnetization values and drag coefficient of MRs must be well adjusted to get the desired result. If the workspace

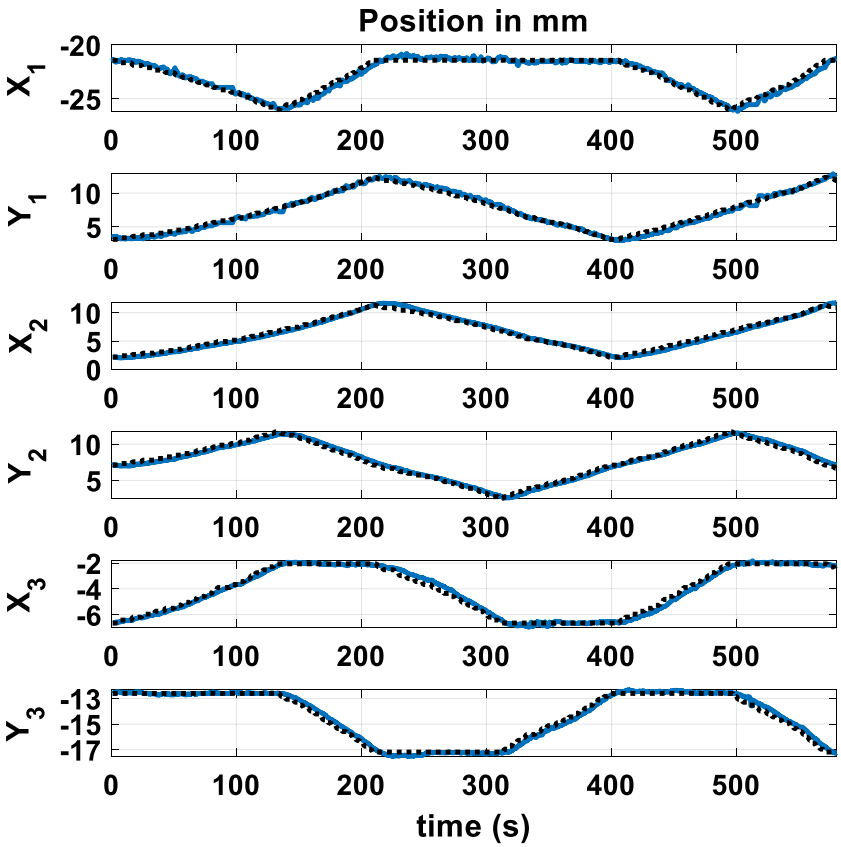

Fig. 11 Actual (blue line) and desired (black dash line) position of microrobots

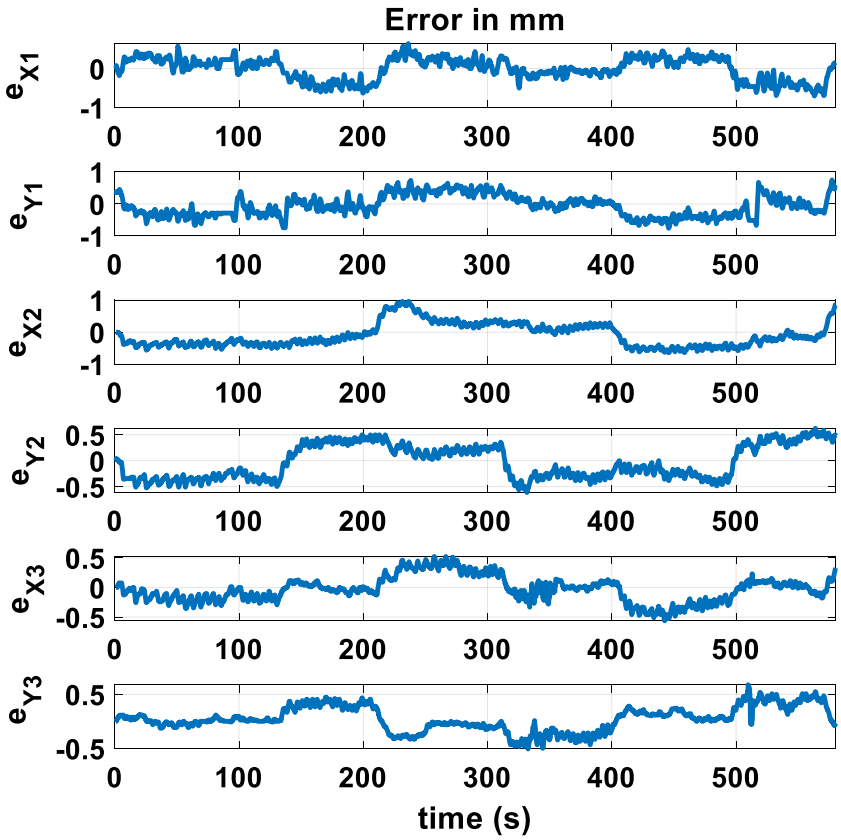

Fig. 12 Position error of microrobots

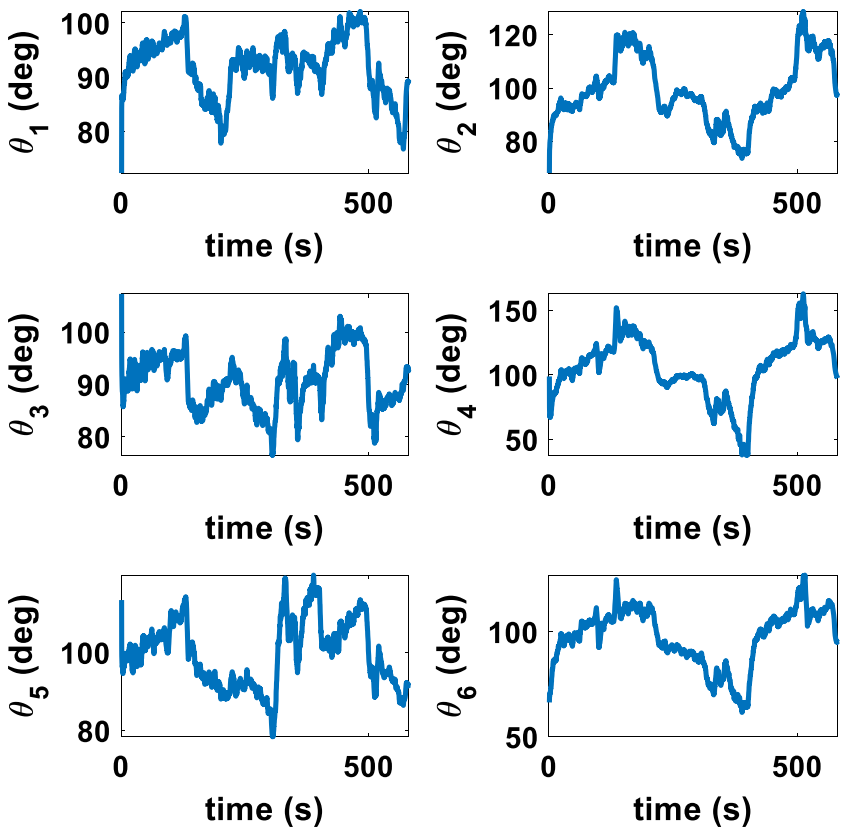

Fig. 13 Permanent magnets rotation angles

is small and the stabilizer MR leaves the region of other MRs, due to the lack of control on this MR (remind that the number of control variables is equal to the system degrees of freedom), the stabilizer MR goes to the corner of the workspace, and does not increase the MRs stability. Videos of the MRs movement in simulations and experiments are provided in the supplementary materials.

5 Conclusion

In this paper, an innovative control strategy based on using a stabilizer microrobot for simultaneous and independent steering of multiple MRs in two dimensions is proposed. The main idea was to employ a stabilizer MR in the workspace to improve the system's stability as well as to reduce control effort. Equations are derived for the general form, with the number of control inputs being equal to the degree of freedom of the system. In the proposed setup $2N$ PMs, as the actuators for generating desired magnetic field, are symmetrically placed around the workspace at equal distances to enable independent control of N MRs. All the MRs in the workspace are also vertically aligned using a Helmholtz coil. To enhance the MRs stability in maintaining their position against external disturbances as well as to improve the control system performance despite model uncertainties, the stabilizer MR is added to the workspace. A PI controller is employed to steer the MRs for tracking desired trajectories. To this aim, required forces on MRs are calculated based on the desired and actual positions, and the PMs angles are obtained from an analytical solution.

Four MRs were controlled with and without stabilizer MRs to evaluate controller performance. The simulation carried out shows the advantages of using the stabilizer MR to improve stability and reduce the control effort, and the effect of various parameters is discussed. In addition, the effectiveness of the proposed system performance for the independent and simultaneous control of three MRs is experimentally demonstrated. A Helmholtz coil and six rotating PMs make up the proposed system. The proper angles of the magnets are calculated analytically by the designed PI controller and applied to the servomotors in each step once the positions

have been determined by the camera. The results show that the proposed control method is effective in successfully controlling MRs independently, as well as in enhancing stability and minimizing control effort.

In this research, we proposed an actuation and control system to steer the motion of the simple microrobots in the presence of the stabilizing microrobot. However, based on the current number of actuators and simple microrobots, it is not possible to control the position of the stabilizer microrobot beside positions of all simple microrobots. Adding more actuators to directly control the position of stabilizer microrobot to improve the controllability of other microrobots holds significant potential as an interesting subject for future research.

Supplementary Information The online version contains supplementary material available at https://doi.org/10.1007/s10846-024-02098-z.

Authors' Contributions Ruhollah Khalesi: Investigation, Algorithms, Simulation, Experimental Implementation, Writing -original draft, Visualization, Data curation.

Hossein Nejat Pishkenari (corresponding author): Conceptualization, Methodology, Writing- Review & Editing, Supervision, Project administration.

Gholamreza Vossoughi: Methodology, Review & Editing, Supervision.

Funding The authors declare that no funds, grants, or other support were received during the preparation of this manuscript.

Code or Data Availability The datasets generated during and/or analyzed during the current study are available from the corresponding author on reasonable request.

Declarations

Ethics Approval We consciously assure that for the manuscript Simultaneous and independent control of multiple swimming magnetic microrobots by stabilizer microrobot the following is fulfilled:
1) This material is the authors' own original work, which has not been previously published elsewhere.
2) The paper is not currently being considered for publication elsewhere.
3) The paper reflects the authors' own research and analysis in a truthful and complete manner.
4) The paper properly credits the meaningful contributions of co-authors and co-researchers.
5) The results are appropriately placed in the context of prior and existing research.
6) All sources used are properly disclosed (correct citation). Literally copying of text must be indicated as such by using quotation marks and giving proper reference.
7) All authors have been personally and actively involved in substantial work leading to the paper, and will take public responsibility for its content.

Consent to Participate Not applicable.

Consent for Publication We give our full permission for the publication.

Competing Interests The authors have no relevant financial or non-financial interests to disclose.

References

1. Chen, W., Fan, X., Sun, M., Xie, H.: The cube-shaped hematite microrobot for biomedical application. Mechatronics **74**, 102498 (2021)
2. Zarrouk, A., Belharet, K., Tahri, O.: Vision-based magnetic actuator positioning for wireless control of microrobots. Robot. Auton. Syst. **124**, 103366 (2020)
3. Chang, X., et al.: Motile Micropump based on synthetic micromotors for dynamic micropatterning. ACS Appl. Mater. Interfaces. **11**(31), 28507–28514 (2019)
4. Rahman, M.A., Cheng, J., Wang, Z., Ohta, A.T.: Cooperative micromanipulation using the independent actuation of fifty microrobots in parallel. Sci. Rep. **7**(1), 1–11 (2017)
5. Chalvet, V., Haddab, Y., Lutz, P.: Trajectory planning for micromanipulation with a nonredundant digital microrobot: shortest path algorithm optimization with a hypercube graph representation. J. Mech. Robot. **8**(2), 021013 (2016)
6. Kong, L., Guan, J., Pumera, M.: Micro-and nanorobots based sensing and biosensing. Curr. Opin. Electrochem. **10**, 174–182 (2018)
7. Kim, K., Guo, J., Liang, Z., Fan, D.: Artificial micro/nanomachines for bioapplications: Biochemical delivery and diagnostic sensing. Adv. Func. Mater. **28**(25), 1705867 (2018)
8. Kim, S., Lee, S., Lee, J., Nelson, B.J., Zhang, L., Choi, H.: Fabrication and manipulation of ciliary microrobots with non-reciprocal magnetic actuation. Sci. Rep. **6**, 30713 (2016)
9. Wang, C., et al.: Review of bionic crawling micro-robots. J. Intell. Rob. Syst. **105**(3), 56 (2022)
10. Pérez-Arancibia, N.O., Duhamel, P.-E.J., Ma, K.Y., Wood, R.J.: Model-free control of a hovering flapping-wing microrobot: the design process of a stabilizing multiple-input–multiple-output controller. J. Intell. Rob. Syst. **77**, 95–111 (2015)
11. Li, D., Liu, C., Yang, Y., Wang, L., Shen, Y.: Micro-rocket robot with all-optic actuating and tracking in blood. Light Sci. Appl. **9**(1), 1–10 (2020)
12. Gao, D., et al.: Optical manipulation from the microscale to the nanoscale: fundamentals, advances and prospects. Light Sci. Appl. **6**(9), e17039 (2017)
13. Ahmed, D., et al.: Rotational manipulation of single cells and organisms using acoustic waves. Nat. Commun. **7**(1), 1–11 (2016)
14. Ozcelik, A., et al.: Acoustic tweezers for the life sciences. Nat. Methods **15**(12), 1021–1028 (2018)
15. Wang, F., Zhao, X., Guo, H., Tian, Y., Zhang, D.: Design of a probe-type acoustic tweezer by acoustic-streaming field optimization. Int. J. Mech. Sci. 107936 (2022). https://doi.org/10.1016/j.ijmecsci.2022.107936

16. Xuan, X.: Recent advances in direct current electrokinetic manipulation of particles for microfluidic applications. Electrophoresis **40**(18–19), 2484–2513 (2019)
17. Zhao, Q., Chen, J., Zhang, H., Zhang, Z., Liu, Z., Liu, S., Di, J., He, G., Zhao, L., Zhang, M., Su, T.: Hydrodynamics modeling of a piezoelectric micro-robotic fish with double caudal fins. J. Mech. Robot. **14**(3), 034502 (2022). https://doi.org/10.1115/1.4052973
18. Yousefi, M., Pishkenari, H.N.: Independent position control of two identical magnetic microrobots in a plane using rotating permanent magnets. J. Micro-Bio Robot. **17**, 59–67 (2021). https://doi.org/10.1007/s12213-021-00143-w
19. Sayyaadi, H., Motekallem, A.: A new propulsion system for microswimmer robot and optimizing geometrical parameters using PSO algorithm. Int. J. Marit. Technol. **8**, 35–45 (2017)
20. Ghanbari, A., Bahrami, M.: A novel swimming microrobot based on artificial cilia for biomedical applications. J. Intell. Rob. Syst. **63**(3–4), 399–416 (2011)
21. Nguyen, K.T., Lee, H.-S., Kim, J., Choi, E., Park, J.-O., Kim, C.-S.: A composite electro-permanent magnetic actuator for microrobot manipulation. Int. J. Mech. Sci. **229**, 107516 (2022). https://doi.org/10.1016/j.ijmecsci.2022.107516
22. Cao, Q., Fan, Q., Chen, Q., Liu, C., Han, X., Li, L.: Recent advances in manipulation of micro-and nano-objects with magnetic fields at small scales. Mater. Horiz. **7**(3), 638–666 (2020)
23. Liu, Y.-L., Chen, D., Shang, P., Yin, D.-C.: A review of magnet systems for targeted drug delivery. J. Control. Release **302**, 90–104 (2019)
24. Khalesi, R., Pishkenari, H.N., Vossoughi, G.: Independent control of multiple magnetic microrobots: design, dynamic modelling, and control. J. Micro-Bio Robot. **16**(2), 215–224 (2020). https://doi.org/10.1007/s12213-020-00136-1
25. Das, S., Steager, E.B., Hsieh, M.A., Stebe, K.J., Kumar, V.: Experiments and open-loop control of multiple catalytic microrobots. J. Micro-Bio Robot. **14**(1–2), 25–34 (2018)
26. Xu, T., Huang, C., Lai, Z., Wu, X.: Independent control strategy of multiple magnetic flexible millirobots for position control and path following. IEEE Trans. Robot. **38**, 2875–2887 (2022)
27. Tung, H.-W., Maffioli, M., Frutiger, D.R., Sivaraman, K.M., Pané, S., Nelson, B.J.: Polymer-based wireless resonant magnetic microrobots. IEEE Trans. Rob. **30**(1), 26–32 (2013)
28. Johnson, B.V., Chowdhury, S., Cappelleri, D.J.: Local magnetic field design and characterization for independent closed-loop control of multiple mobile microrobots. IEEE/ASME Trans. Mechatron. **25**(2), 526–534 (2020)
29. Hsu, A., Zhao, H., Gaudreault, M., Foy, A.W., Pelrine, R.: Magnetic milli-robot swarm platform: a safety barrier certificate enabled, low-cost test bed. IEEE Robot. Autom. Lett. **5**(2), 2913–2920 (2020)
30. Dong, X., Sitti, M.: Controlling two-dimensional collective formation and cooperative behavior of magnetic microrobot swarms. Int. J. Robot. Res. **39**(5), 617–638 (2020)
31. Denasi, A., Misra, S.: Independent and leader–follower control for two magnetic micro-agents. IEEE Robot. Autom. Lett. **3**(1), 218–225 (2017)
32. Wong, D., Steager, E.B., Kumar, V.: Independent control of identical magnetic robots in a plane. IEEE Robot. Autom. Lett. **1**(1), 554–561 (2016)
33. Ongaro, F., Pane, S., Scheggi, S., Misra, S.: Design of an electromagnetic setup for independent three-dimensional control of pairs of identical and nonidentical microrobots. IEEE Trans. Rob. **35**(1), 174–183 (2018)
34. Khalesi, R., Yousefi, M., Pishkenari, H.N., Vossoughi, G.: Robust independent and simultaneous position control of multiple magnetic microrobots by sliding mode controller. Mechatronics **84**, 102776 (2022)
35. Salehizadeh, M., Diller, E.: Three-dimensional independent control of multiple magnetic microrobots via inter-agent forces. Int. J. Robot. Res. **39**(12), 1377–1396 (2020). https://doi.org/10.1177/0278364920933655
36. Ryan, P., Diller, E.: Magnetic actuation for full dexterity microrobotic control using rotating permanent magnets. IEEE Trans. Rob. **33**(6), 1398–1409 (2017)
37. Petruska, A.J., Abbott, J.J.: Optimal permanent-magnet geometries for dipole field approximation. IEEE Trans. Magn. **49**(2), 811–819 (2012)
38. Happel, J., Brenner, H.: Low Reynolds number hydrodynamics: with special applications to particulate media. Springer Science & Business Media (2012)

Ruhollah Khalesi received his B.Sc., M.Sc., and Ph.D. degrees in Mechanical Engineering from the Sharif University of Technology in 2012, 2014 and 2022, respectively. His-current research interests include Control and Robotics.

Hossein Nejat Pishkenari earned his B.Sc., M.Sc., and Ph.D. degrees in Mechanical Engineering from the Sharif university of Technology in 2003, 2005 and 2010, respectively. Then he joined the Department of Mechanical Engineering at the Sharif University of Technology in 2012. Currently, he is directing the Nanorobotics Laboratory. One of his main research interests is Dynamics and Control of Micro/Nano Robots.

Gholamreza Vossoughi received his Ph.D. from Mechanical Engineering Dept. at University of Minnesota in 1992. Ever since he has been a faculty member of Mechanical Engineering Dept. at Sharif University of Technology. He has served as the Manufacturing Engineering and Applied Mechanics Division Directors from 1994 to 1998 and as the Graduate Dean of the Mechanical Engineering from 1999 to 2003.